Journal of Molecular Catalysis A: Chemical 316 (2010) 30–44

Contents lists available at ScienceDirect

Journal of Molecular Catalysis A: Chemical

journal homepage: www.elsevier.com/locate/molcata

Transesterification reaction of triglycerides in the presence of Ag-doped $H_3PW_{12}O_{40}$

A. Zieba, L. Matachowski, J. Gurgul, E. Bielańska, A. Drelinkiewicz*

Institute of Catalysis and Surface Chemistry Polish Academy of Sciences, 30-239 Kraków, Niezapominajek 8, Poland

ARTICLE INFO

Article history:
Received 17 June 2009
Received in revised form
25 September 2009
Accepted 28 September 2009
Available online 4 October 2009

Keywords:
Biodiesel
Transesterification
Triacetin
Castor oil
Heteropolyacid

ABSTRACT

Present work is concerned with examination of catalytic properties of 12-tungstophosphoric acid and its silver salts $Ag_xH_{3-x}PW_{12}O_{40}$ with Ag-content ranging from $x = 0.5$ up to $x = 3$ for transesterification of triglycerides with methanol to form methyl ester (biodiesel) under mild conditions (atmospheric pressure, temperature of 50–60 °C). Reaction was studied for triacetin, a model triglyceride and for vegetable oil, castor oil. Various techniques (BET, FTIR, XRD, XPS, laser diffraction, electron microscopy, SEM, and EDS) were used to characterize as-received Ag-salts and the samples separated after the catalytic tests. Because of the presence of methanol, which is the reactant, silver salts formed colloidal dispersion during the catalytic reaction. Under such conditions, all silver salts were active for transesterification of triglycerides. The conversion of triglycerides gradually decreases as the protons in heteropolyacid are replaced by Ag^+ cations. However, due to the leaching of parent $H_3PW_{12}O_{40}$ upon dissolving in methanol, the contribution of homogeneous catalysis was observed, especially in the presence of Ag-salts with low silver content such as $Ag_{0.5}H_{2.5}PW_{12}O_{40}$. Catalytic performance of Ag-salts in methanolysis of a short-chain triglyceride, triacetin, differs remarkably from that in castor oil comprising natural, long-chain triglycerides. After transesterification of castor oil, initially crystalline particles of Ag-salts partially rearrange to "gel-type" material making their further processing difficult. Although, no "gel-type" particles are formed after reaction of triacetin, the formation of "nanowires" due to partial reduction of some of Ag^+ ions is observed.

1. Introduction

Biodiesel, a nonpetroleum-based fuel consists of fatty acid methyl-esters (FAME) formed through a transesterification reaction. In this process, the triglycerides of fatty acids (C_{14}–C_{20}) from renewable sources like vegetable oils, animal fats and recycled greases from food industry are converted to methyl-esters and glycerol as a by-product in transesterification reaction with methanol (methanolysis). The reaction has traditionally been catalysed by homogeneous catalysts, such as K- or Na-alkoxides or -hydroxides, and mineral acids [1–3]. However, the application of heterogeneous catalysts is more desirable from economic, technological and environmental points of view. In particular, solid acid catalysts seem to be very useful since they are able to catalyse both the transesterification of triglycerides and esterification of free fatty acids, which becomes important when using recycled greases. Therefore, great research efforts have recently been undertaken to find efficient solid acid catalysts and the results of these studies were reviewed in general papers [1–3].

The most commonly tested vegetable oils include palm oil, soybean oil, sunflower oil, coconut oil and rapeseed oil. Moreover, castor oil derived from *Riccinus communis* plants is mentioned frequently in the literature as a potential raw material for biodiesel. The main constituent of castor oil is triglyceride of 12-hydroxy-9-octadecenoic acid (ricinoleic acid, Scheme 1). Due to the presence of OH group at C-12 carbon, castor oil exhibits unique chemical and physical properties. Castor oil is well soluble in both methanol and methyl-esters formed and the homogeneity of reaction mixture is attained during transesterification reaction [4–6].

It is well known that Keggin type heteropolyacids and their acidic salts are useful catalysts for reactions requiring strong acidity. Although they are useful solid catalysts for gas-phase reactions, they are highly soluble in polar media like water and methanol. Therefore, when studied in methanolysis of rapeseed oil, heteropolyacids ($H_3PW_{12}O_{40}$, $H_4SiW_{12}O_{40}$, and $H_3PMo_{12}O_{40}$) acted as homogeneous catalysts and their activity was higher than those of mineral acids (H_2SO_4 and H_3PO_4) [7]. However, quite recently published data demonstrated that heteropolyacids ($H_3PW_{12}O_{40}$ and $H_3PMo_{12}O_{40}$) supported on acid-treated K-10 clay were effective and stable catalysts in the transesterification of different oils with alcohols [8]. On the other hand, by combining various amounts of heteropolyacid $H_3PW_{12}O_{40}$ and large monovalent

* Corresponding author.
E-mail address: ncdrelin@cyf-kr.edu.pl (A. Drelinkiewicz).

1381-1169/$ – see front matter © 2009 Elsevier B.V. All rights reserved.
doi:10.1016/j.molcata.2009.09.019

cations such as NH_4^+, K^+, Cs^+ and Ag^+ microporous solid acidic catalysts were obtained. They were highly effective in a number of catalytic reactions including isomerization, hydration, alkylation, hydrolysis, and esterification [9–13]. Catalytic efficiency of Cs- and K-salts of heteropolyacids was also evaluated for transesterification of triglycerides [13–17]. For instance, cesium salts $Cs_xH_{3-x}PW_{12}O_{40}$ with various Cs content (x = 0.9–3) were found to be effective catalysts in methanolysis of tributyrin, a model compound of natural triglycerides [13]. Their activity increased with an increase of Cs content up to x = 2.0–2.3, and then dropped rapidly. Two salts $Cs_{2.5}H_{0.5}PW_{12}O_{40}$ and $Cs_2HPW_{12}O_{40}$ turned out to be effective acid catalysts for the transesterification of vegetable oil (*Eruca sativa Gars*) [14] and rapeseed oil [15], respectively. Cs-doped $H_4SiW_{12}O_{40}$ catalyst was found to be active in transesterification of model C_4 and C_8 triglycerides and esterification of palmitic acid [16]. In our previous work Cs- and K-salts of $H_3PW_{12}O_{40}$ were studied in methanolysis of castor oil [17]. In the reaction mixture they formed colloidal dispersion. This resulted in much higher activity of K-salts when compared to that of their Cs-analogous. Moreover, the NH_4^+, K^+ and Cs^+ salts of HPW were found to be effective catalysts in esterification of palmitic acid [16,18,19].

On the other hand, markedly less attention was directed to catalytic properties of insoluble silver salts of $H_3PW_{12}O_{40}$. Literature data show that due to the presence of acidic protons and Ag^+ cations they can act as bifunctional catalysts. This type of bifunctional activity was observed by Moffat and co-workers in a ring-expansion of methylcyclopentane and ring-contraction of cyclohexane [20]. Furthermore, such bifunctionality was noticed by Haber et al. in hydration of ethylene and dehydration of ethanol [21]. Catalytic activity of Ag-salts of $H_3PW_{12}O_{40}$ caused by the acidic centres was observed in dehydration of the 1-, 2- and tert-butyl alcohols [22]. In all these reactions gaseous reactants were used whereas Ag-salts acted as the solid catalysts (gas-phase reactions). Quite recently, Yadav et al. [23] reported that $Ag_3PW_{12}O_{40}$ was mild and selective acid catalyst in the synthesis of β-ketoesters via C–H insertion, reaction performed in liquid phase using dichloromethane as the solvent.

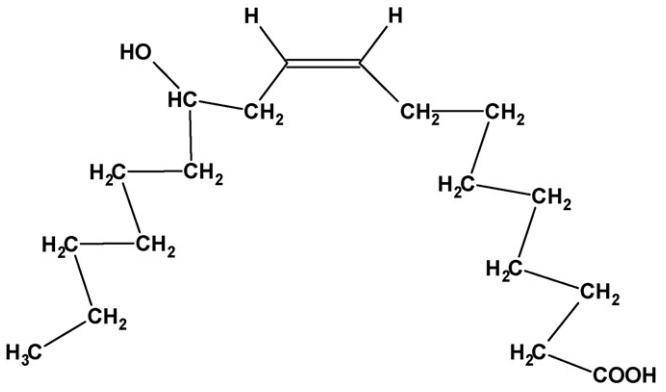

Scheme 1. Ricinoleic acid.

In the present work, silver salts $Ag_xH_{3-x}PW_{12}O_{40}$ with various Ag-content ranging from x = 0.5 up to x = 3 are studied. Their catalytic properties are evaluated for transesterification of triglycerides by methanol, i.e. in reaction performed in highly polar medium. Reaction is studied for triglycerides, namely castor oil and triacetin. The methanolysis of triacetin (the acetic acid triester of glycerol) which is the simplest triglyceride has already been studied as a model reaction for the transesterification of natural oils [24–29]. Triacetin exhibits the same chemical functionality of any triglyceride molecule and shares the same reactivity

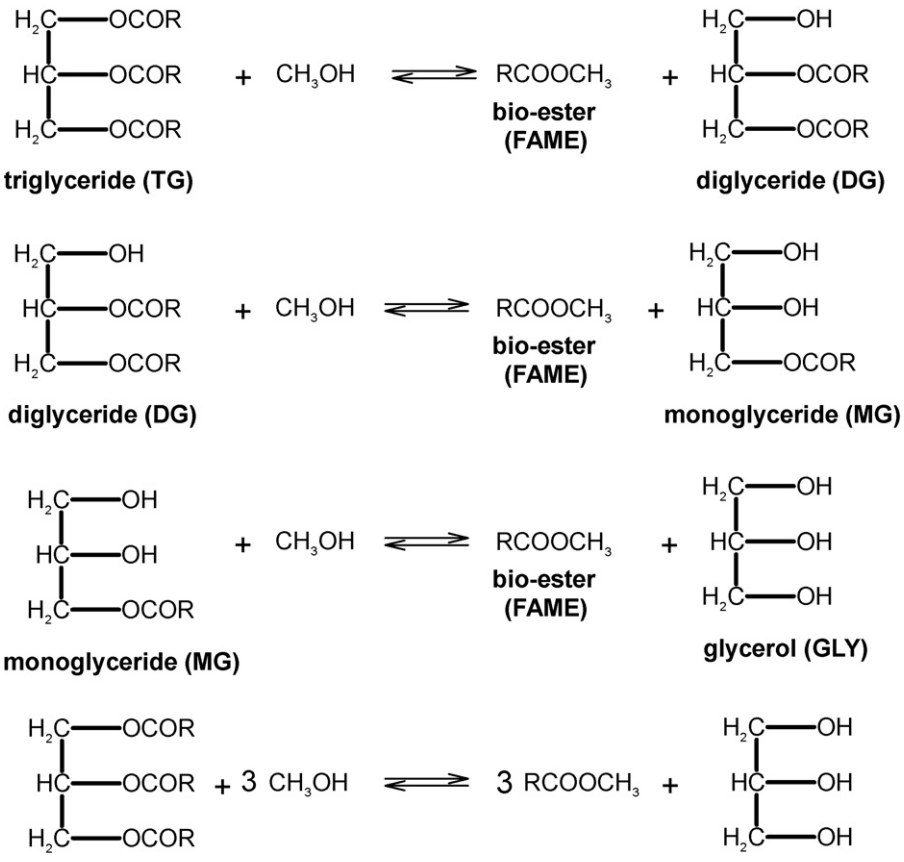

Scheme 2. Tranesterification of triglyceride with methanol.

principles of triglycerides. Its methanolysis is accomplished via three sequential steps, similarly to the methanolysis of other triglycerides (Scheme 2). Reaction proceeds via the intermediate products, diacetin and monoacetin to produce finally methyl acetate and glycerol. Here, by using short-chain (triacetin) and long-chain triglycerides (triglyceride of ricinoleic acid in castor oil), the effect of the triglyceride on its transesterification reactivity is compared in the presence of soluble $H_3PW_{12}O_{40}$ and its silver salts. It should be stressed that castor oil and triacetin are readily soluble in methanol and methyl-esters formed in reactions. This has not been observed yet for commonly used natural oils. Thus, in methanolysis of both our triglycerides, there is a single liquid-phase system and no other separate phases of methanol and triglycerides appear. Therefore mass-transfer effects resulting from the presence of two phases (oil–methanol) encountered during transesterification of natural oils with methanol may be neglected.

2. Experimental

2.1. Catalysts preparation

Commercially available 12-tungstophosphoric acid ($H_3PW_{12}O_{40}$, HPW, Merck) was used to prepare silver salts. Prior to the salts preparation, the sample of HPW was analyzed by DTG method to determine the content of water. The silver salts $Ag_xH_{3-x}PW_{12}O_{40}$ with Ag-content from $x = 0.5$ up to $x = 3$ (abbreviated in the text as $Ag_{0.5}H_{2.5}PW_{12}O_{40}$–Ag-0.5; $Ag_2HPW_{12}O_{40}$–Ag-2) were prepared by precipitation method, following the procedure described in detail previously [21].

The stoichiometric quantities of $AgNO_3$ solution (0.04 M) were added to aqueous solutions of the 12-tungstophosphoric acid (0.10 M). The preparations were performed at ambient temperature without stirring. The resulting white colloidal solutions of silver salts were left overnight in the oven at 40 °C to slowly evaporate to dryness.

2.2. Characterization of catalysts

The specific surface areas of samples were calculated from the nitrogen adsorption–desorption isotherms at 77 K in an Autosorb-1 Quantachrome instrument. Prior to the measurements, the samples were preheated and degassed under vacuum at 200 °C for 2 h.

FTIR studies were carried out using Bruker-Equinox 55 spectrometer and standard KBr pellets technique.

X-ray diffraction (XRD) patterns were obtained with a Siemens D5005 diffractometer using Cu Kα radiation (55 kV, 30 mA). The samples were dried at 120 °C before the measurement.

The X-ray photoelectron spectroscopy (XPS) measurements were carried out with a hemispherical analyzer (SES R4000, Gammadata Scienta). The unmonochromatized Al Kα (1486.6 eV) X-ray source with the anode operating at 12 kV and 20 mA current emission was applied to generate core excitation. The base pressure in the analysis chamber was about 8×10^{-9} Pa and about 1×10^{-7} Pa during experiment. The energy resolution of the system, measured as a full width at half maximum (FWHM) for Ag $3d_{5/2}$ excitation line, was 0.9 eV. All binding energy values were charge-corrected to the carbon C 1s excitation which was set at 285.0 eV. The powder samples were pressed into indium foil and mounted on a special holder. The area of sample analysis was about 3 mm^2. All spectra were collected at pass energy of 100 eV except survey scans which were collected at pass energy of 200 eV. Intensities were estimated by calculating the integral of each peak, after subtraction of the Shirley-type background, and fitting the experimental curve with a combination of Gaussian and Lorentzian lines of variable proportions (70:30). The accuracy of the XPS analysis is approximately 3%. The Ag 3d peaks were deconvoluted into a few peaks components taking into account a spin–orbit splitting of 6.0 eV and relative intensity ratio of the $3d_{5/2}$ to $3d_{3/2}$ peaks equal to 1.5.

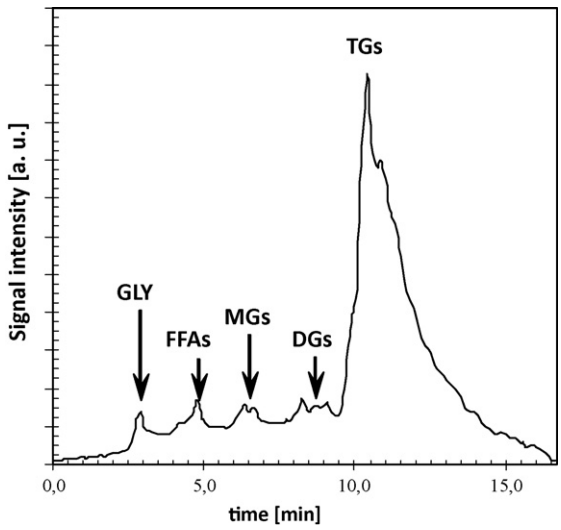

Fig. 1. HPLC chromatogram for castor oil (*Abbreviations*: GLY – free glycerol, FFAs – free fatty acids, MGs – mono-glycerides, DGs – diglycerides, TGs – triglycerides).

Electron microscopy studies were performed by means of Field Emission Scanning Electron Microscope JEOL JSM – 7500 F. Energy dispersive X-ray (EDS) measurements were performed taking into account the Ag and W elements.

The size distribution of Ag-2 salt particles in the colloidal dispersion was analyzed using Laser Diffraction Particle Size Analyzer LS 13 320 (Beckman Coulter Inc.). In experiments, the mixture methanol–triacetin (initial molar ratio of 29:1) of the same composition to that in methanolysis reaction was used. The measurements were carried out at 25 °C and subsequently after heating the mixture to 35 °C, 45 °C and 55 °C, respectively. The sizes of particles were measured in the range of 40 nm to 4000 nm.

2.3. Catalytic tests

The transesterification of triglycerides, triacetin, and castor oil with methanol was carried out in a 100 cm^3 glass reactor at atmospheric pressure following the procedure described in our previous paper [17]. Reactor was equipped with a reflux condenser, magnetic stirrer, and a tube for sampling the solution. For all reactions, the initial molar ratio of methanol to triglycerides (castor oil or triacetin) equal to 29:1 was used. Prior to the catalytic tests all the Ag-samples were ground into powder and dried at 120 °C in order to remove crystallization water.

Methanolysis of castor oil was performed using 6 g of castor oil (Microfarm, Poland), 7.6 cm^3 of methanol (Fluka), and 0.5 g of Ag-salts. This composition corresponded to molar ratio of methanol/oil/catalyst equal to 29/1/0.025. In catalytic experiment, castor oil, methanol and internal standard (eicosane) were introduced to the reactor, heated up to 60 °C and then the catalyst was added. Typically, methanolysis was carried out for 3 h at 60 °C and the samples were withdrawn at appropriate time intervals. The progress of reaction was studied by means of HPLC and GC techniques. The procedure of HPLC method was described before [17]. The composition of initial castor oil was determined by HPLC method. Furthermore, in selected catalytic experiments the change in concentration of castor oil during the methanolysis reaction was determined by HPLC method.

The HPLC chromatogram (Fig. 1) shows that our castor oil is entirely composed (ca. 90%) of triglyceride of ricinoleic acid. How-

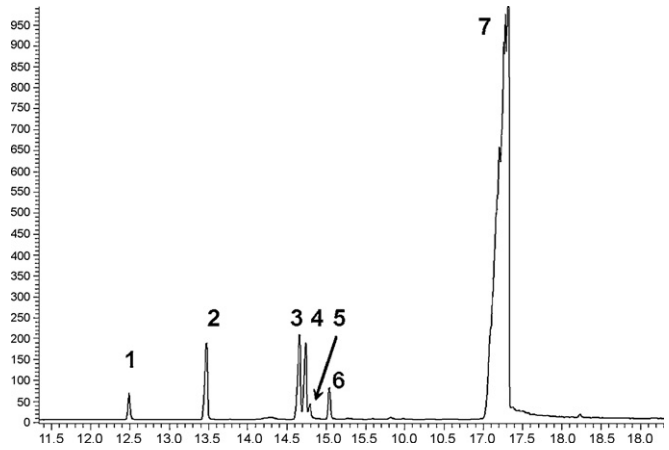

Fig. 2. GC chromatogram of methyl-esters obtained in methanolysis of castor oil (1 – methyl palmitate, 2 – internal standard (eicosane), 3 – methyl linoleate, 4 – methyl oleate, 5 – methyl linolenate, 6 – methyl stearate, 7 – methyl ricinoleate).

ever, apart from triglyceride, castor oil contains trace amounts of di- and mono-glycerides of ricinoleic acid, glycerol and free ricinoleic acid. By using analytical standard, the content of free ricinoleic acid was determined to be below 0.1 wt%.

The content of free glycerol in castor oil was estimated by the method described by Naviglio et al. [30]. In the method, glycerol was quantitatively and specifically oxidized into formic acid by adding sodium metaperiodate solution according to the reaction:

$$C_3H_8O_3 + 2NaIO_4 = 2NaIO_3 + 2CH_2O + HCOOH + H_2O$$

Then, the content of formic acid which is equivalent to the content of glycerol was determined by an acid–base titration in the presence of phenolphthalein as pH indicator. Using this procedure, the content of free glycerol in our castor oil was determined to be very low, below 0.1 wt%, which quite well agrees with the quantity of glycerol evaluated by HPLC method.

The composition of methyl-esters formed in methanolysis of castor oil was determined by GC technique using analytical procedure described before [17]. The analysis was performed with a gas chromatograph PE Clarus 500 equipped with a flame ionisation detector under conditions: capillary column Elite-5 MS (30 m × 0.25 mm × 0.25 μm coating) with helium as a carrier gas (flow rate 1 ml/min) and injection temperature 260 °C. Product separation was obtained using temperature ramps: 120 °C for 1 min, 10 °C/min to 180 °C, 7 °C/min to 260 °C and held at 260 °C for 15 min.

For GC analysis the sample of reaction mixture (40 μl) withdrawn from the reactor was added to 1 cm^3 of hexane. Then, the mixture was shaken to separate the catalyst and the solution obtained after filtration was analyzed by GC method. A sample (1 μl) of this solution was injected to GC, and the content of methyl-esters (FAME) was quantified using an internal standard method. As described before [17] the yield of methyl-esters formed in methanolysis of castor oil was expressed in terms of the percentage of methyl-esters produced.

A representative GC chromatogram of methyl-esters obtained in methanolysis of our castor oil is reported in Fig. 2, and the content of methyl-esters determined by GC in Table 1. It can be seen that bio-esters are composed entirely of methyl ricinoleate (87.44 wt%) and they contain only traces of fatty acids methyl-esters. Thus, the composition of our castor oil is practically the same as that reported by other authors [6,31]. Molecular weight of 928 g/mol for castor oil was assumed.

The transesterification of triacetin with methanol (1:29 molar ratio) was performed at 50 °C using the concentration of catalysts equal to 0.00225 mol/dm^3. In the course of catalytic tests the samples of reaction mixture were periodically withdrawn and analyzed by GC method using toluene as internal standard. Then, 40 μl of the sample taken from reactor was added to 1 cm^3 of THF, and 1 μl of the obtained solution was injected to GC (PE Clarus 500 equipped with a flame ionisation detector, capillary column Elite-5 MS (30 m × 0.25 mm × 0.25 μm coating) with helium as a carrier gas (flow rate 1 ml/min) and injection temperature 260 °C). Product separation was achieved using temperature ramps 50 °C for 1 min, 3 °C/min to 65 °C, 30 °C/min to 260 °C, and held at 260 °C for 2 min. The response factors for triacetin, diacetin (Aldrich), monoacetin (Acros Organics) and methyl acetate (Aldrich) were determined through multipoint calibrations of standards.

For the microscopic studies (SEM) the samples were separated from the reaction mixture by centrifugation. The separation by simple filtration was impossible because of the presence of very small colloidal particles in the reaction mixture.

Table 1
Composition of methyl-esters (FAME) derived from castor oil, determined by GC method.

Methyl-ester	Number of C atoms/number of C=C bonds	Content [wt%]
Methyl ricinoleate	C18:1, 1-OH	87.44
Methyl linoleate	C18:2	5.05
Methyl oleate	C18:1	3.88
Methyl stearate	C18:0	1.40
Methyl palmitate	C16:0	1.28
Methyl linolenate	C18:3	0.56
Others		0.39

3. Results and discussion

In the first part of the work, silver salts $Ag_xH_{3-x}PW_{12}O_{40}$ of Ag-content ranging from $x = 0.5$ to $x = 3$ are studied in methanolysis of triacetin, a short-chain triglyceride which is a model compound for natural triglycerides. In the second part, their reactivity is compared to that determined for natural triglyceride, castor oil consisting of long-chain triglycerides.

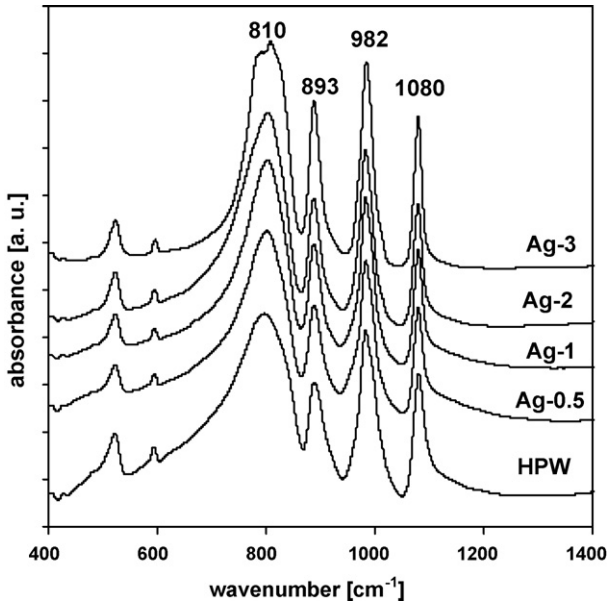

Fig. 3. FTIR spectra of pure $H_3PW_{12}O_{40}$ and Ag-salts of various Ag-content.

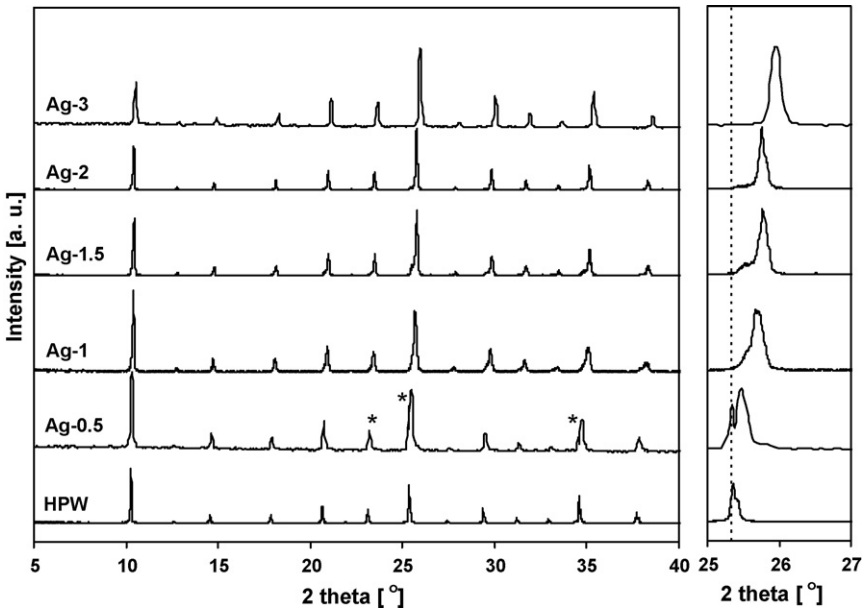

Fig. 4. Powder X-ray diffraction patterns of parent $H_3PW_{12}O_{40}$ acid and Ag-salts.

3.1. Characterization of Ag-salts of $H_3PW_{12}O_{40}$

The structures and morphologies of Ag-salts were studied by means of FTIR, powder X-ray diffraction (XRD), X-ray photoelectron spectroscopy (XPS), scanning electron microscopy (SEM), and X-ray energy dispersive spectroscopy (EDS) techniques.

3.1.1. FTIR spectroscopy

The FTIR spectra of Ag-salts and of parent $H_3PW_{12}O_{40}$ are displayed in Fig. 3. In the spectrum of HPW the bands characteristic of Keggin anions can clearly be seen. They are the bands located at 1080 (ν_{as} P–O_a, oxygen in the central PO_4 tetrahedron), 982 cm^{-1} (W–O_d, terminal oxygen bonding to W atom), 893 cm^{-1} (ν_{as} W–O_b–W, edge-sharing oxygen connecting W) and 810 cm^{-1} (W–O_c–W, corner-sharing oxygen connecting W_3O_{13} units) [32]. All these bands also appear in the spectra of all Ag-salts. Their positions do not change referred to those in the spectrum of parent HPW. This indicates that the structure of Keggin anions of $H_3PW_{12}O_{40}$ does not change when the protons are replaced by the silver cations.

3.1.2. XRD diffraction

The XRD diffraction patterns of silver salts of various Ag-content and of $H_3PW_{12}O_{40}$ are displayed in Fig. 4. The diffraction pattern of the parent HPW coincides with the XRD data reported for the hexahydrated $H_3PW_{12}O_{40} \times 6H_2O$ corresponding to a cubic Pn3m crystalline structure [32]. According to the literature, silver salts of HPW posses the same cubic symmetry but with a contracted unit cell [21,32]. It has been established that with the increase of Ag-content the lattice parameters gradually decreased from a_0 = 12.5 Å for $H_3PW_{12}O_{40} \times 6H_2O$ to a_0 = 11.8 Å for Ag-3 salt [21,33]. Therefore, for Ag-salts the reflexes assigned to the Keggin salts were shifted in comparison to those of pure HPW towards higher angle. This was explained by the formation of one crystalline phase of the salts [21].

This effect is also observed in the diffraction pattern of present Ag-samples (Fig. 4). Thus, our X-ray diffraction patterns are consistent with previous data [21] showing only one phase of Ag-salts with good crystallinity when silver content $x > 1$. However, this is not the case for salt with low Ag-content such as Ag-0.5. In the diffraction pattern of Ag-0.5 salt apart from the new reflexes originating from the crystalline phase of silver salt, the reflexes from crystalline phase of parent $H_3PW_{12}O_{40}$ can easily be recognized. This indicates that Ag-0.5 sample is two-phase mixture consisting of silver salt and crystalline HPW.

3.1.3. Microscopic studies (SEM, EDS)

The morphology of initial salts and the samples separated after methanolysis of both triglycerides triacetin and castor oil was studied by means of electron microscopy technique (SEM). Their compositions were examined by energy dispersive X-ray technique (EDS). X-ray microprobe analysis for W and Ag elements was performed in various surface areas of samples. From the contents of W and Ag elements determined in at.%, the molar ratios of W/Ag were calculated.

The micrographs of as-prepared Ag-0.5, Ag-1 and Ag-2 salts are displayed in Figs. 5–7, respectively. It can be seen that all as-received salts are in the form of well-shaped crystalline particles. The smallest crystallites are formed by Ag-0.5 salt (Fig. 5). When the content of silver in the $H_3PW_{12}O_{40}$ increases, the size of crystalline particles evidently grows. As a result, Ag-2 salt forms well-shaped crystallites (Fig. 7) of bigger sizes than those of Ag-0.5. Surprisingly, further increase in the Ag-content leading to fully exchanged Ag-3 salt resulted in the formation of very fine crystalline particles (Fig. 8) of diameters similar to those of Ag-0.5.

The values of W/Ag ratios calculated from the EDS data are collected in Table 2. In the Ag-0.5 salt, the distribution of Ag and W elements was highly non-homogeneous. Some surface areas exhibited higher content of Ag than the others. As a consequence, the W/Ag ratios changed from 3 to 11.5 and are distinctly smaller than W/Ag = 24 calculated from the stoichiometry of the Ag-0.5 salt.

Similar effect can be observed for Ag-1 sample. The average value of W/Ag ratio determined by EDS is about 6, i.e. almost two times less than the stoichiometric ratio W/Ag = 12. Thus, EDS results support the observations obtained from the XRD diffraction pattern (Fig. 4) for Ag-0.5 suggesting that this sample is most probably composed of crystalline HPW and silver salts. Although no crystalline phase of parent HPW was observed by XRD for sample with higher Ag-content, i.e. Ag-1, too low value of W/Ag ratio may indicate that Ag-1 salt is also composed of HPW and crystalline Ag-salts. The presence of amorphous HPW and/or small cluster of HPW, too small to be detected by XRD cannot be excluded.

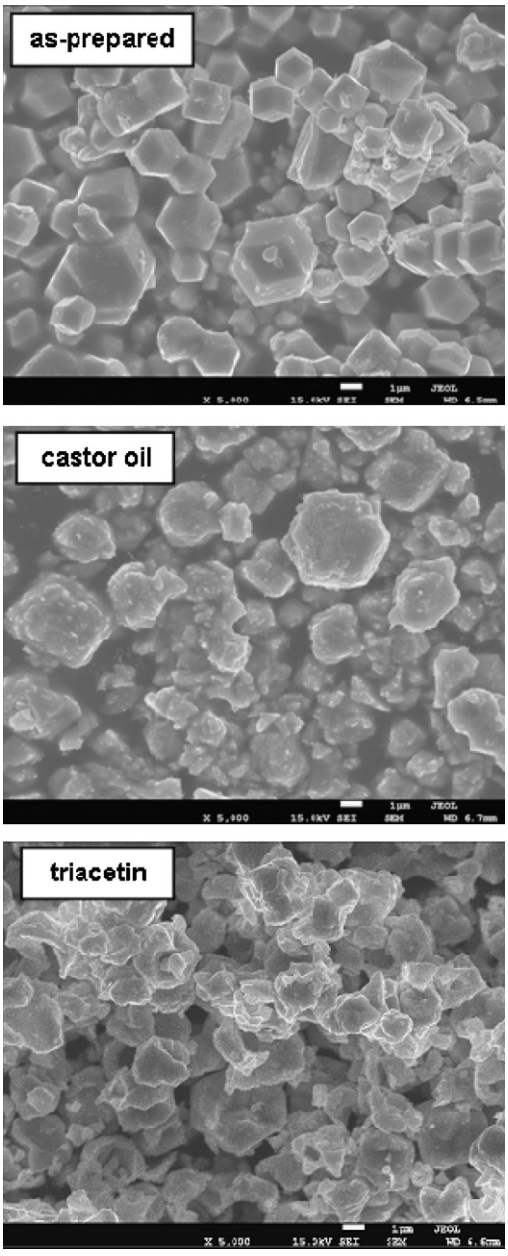

Fig. 5. Scanning electron micrographs of initial Ag-0.5 salt and the precipitate after methanolysis of castor oil or triacetin.

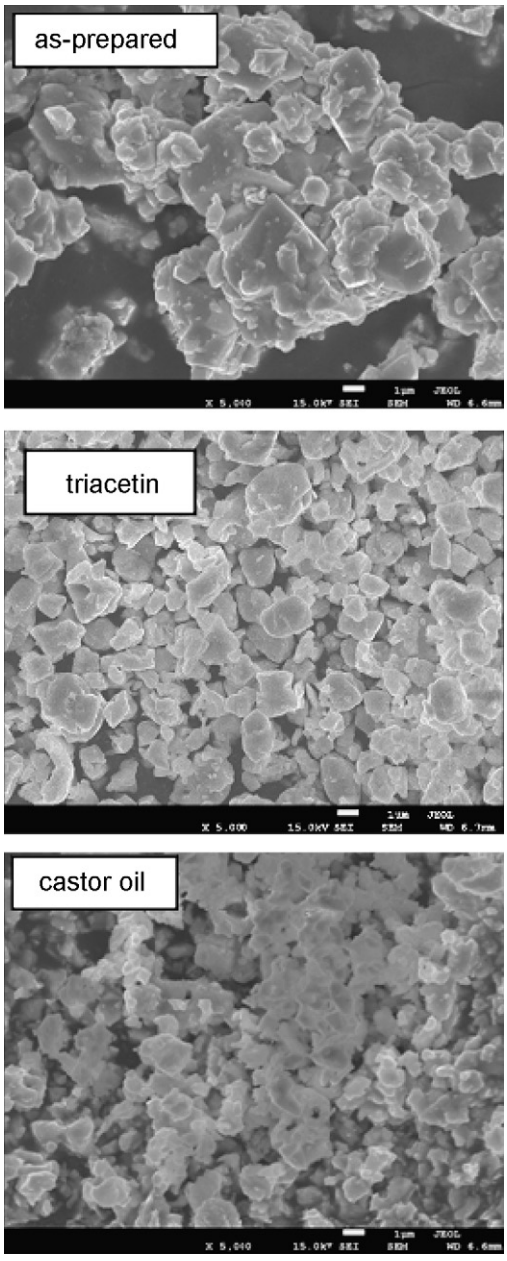

Fig. 6. Scanning electron micrographs of initial Ag-1 salt and the precipitate after methanolysis of triacetin and castor oil.

Table 2
Energy dispersive X-ray (EDS) analysis data for Ag and W in Ag-salts of $H_3PW_{12}O_{40}$, initial Ag-salts and solids obtained after methanolysis of castor oil or triacetin.

Sample	W/Ag stoichiom.		W/Ag determined by EDS	W/Ag average value from EDS
Ag-0.5	24	As-prepared	4.1; 8.4; 3.0; 7.1; 11.5	
		After reaction of triacetin	5.0; 7.8; 6.5; 4.4	5.9
		After reaction of castor oil	12; 9.0; 16.2; 3.2; 2.8; 7.3	
Ag-1	12	As-prepared	6.7; 5.5	6.1
		After reaction of triacetin	6.8; 4.4; 4.5; 4.8; 5.2	5.13
		After reaction of castor oil	4.0; 4.7; 4.3; 4.1; 4.15; 4.1	4.23
Ag-2	6	As-prepared	5.4; 6.7; 4.8; 6.7	5.9
		After reaction of triacetin	3.4; 3.3; 2.0[a]; 1.7[a]	
		Treated by CH_3OH	6.4; 5.3; 5.3; 4.7; 4.7	
Ag-3	4	As-prepared	5.1; 4.3	4.75
		Treated by CH_3OH	4.7; 4.8; 4; 6.3; 3.8[b], 2.5[b]	

[a] EDS analysis in the area with "nanowires", marked in Fig. 7.
[b] EDS analysis in the area of morphological changes, marked in Fig. 8.

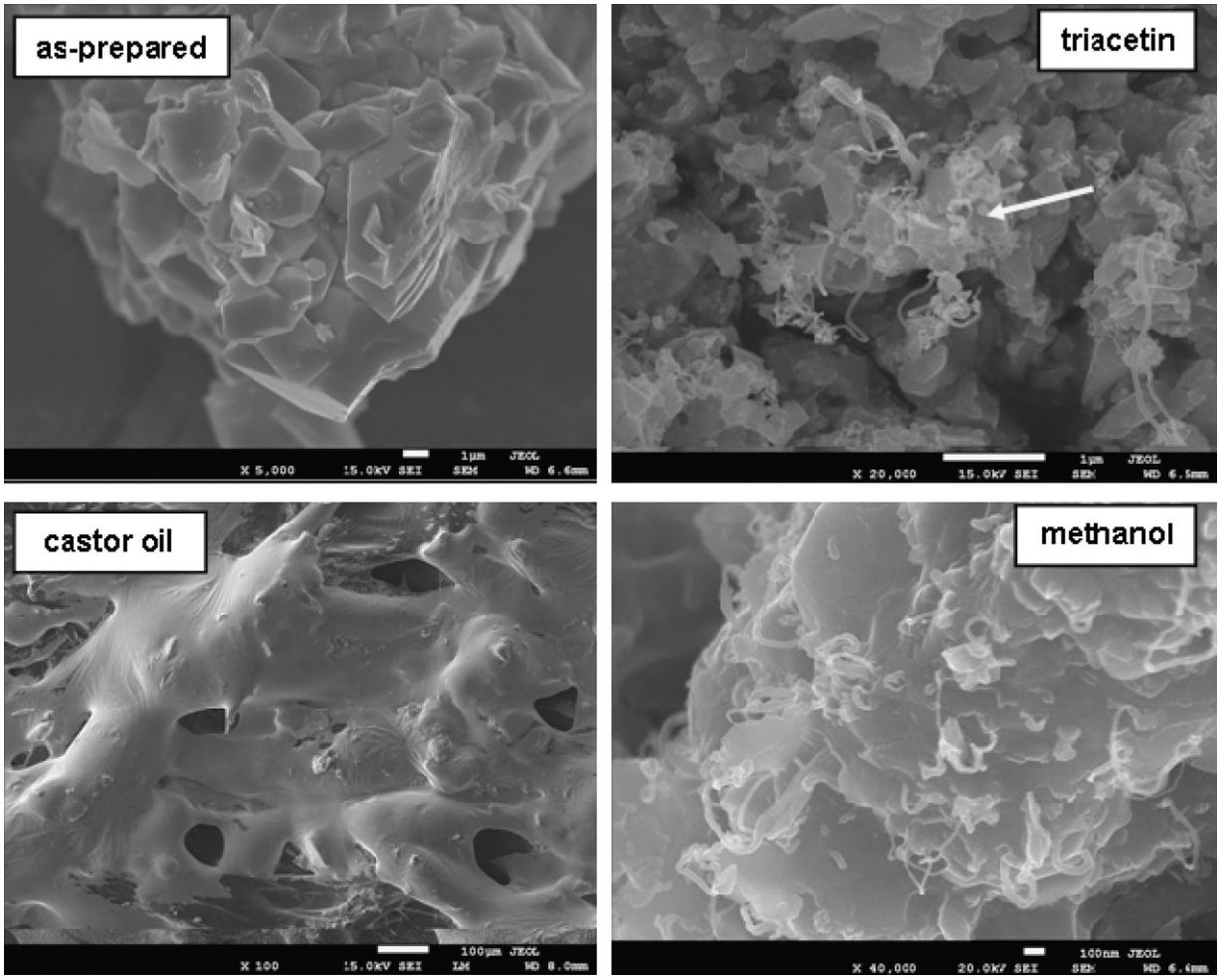

Fig. 7. Scanning electron micrographs of initial Ag-2 salt and the precipitate after methanolysis of triacetin, castor oil and treated by methanol.

On the other hand, for Ag-2, Ag-2.5 and Ag-3 salts the W/Ag ratios calculated from the EDS analysis are close to the stoichiometric values. For instance, the average value of W/Ag for Ag-2 salt calculated as 5.9 is very close to the stoichiometric W/Ag = 6 (Table 2). This observation is consistent with the XRD diffraction pattern (Fig. 4) revealing the presence of one crystalline phase for Ag-2 salt.

As shown in Table 3, all Ag-salts exhibit very small values of specific surface areas, they do not exceed 5 m^2/g. According to the literature reports [32,33] small surface areas were measured for silver salts prepared by evaporation procedure. This procedure was used in present work. As pointed out by Parent and Moffat [33] precipitation of salts in the presence of a deficit of Ag^+-cation (relative to the stoichiometric Ag-3 composition) would presumably trap the residual protons within the crystallographic structure, consequently leading to a blocking of the micropores and hence decreasing surface areas. This phenomenon could be perceived as the formation of a solid solution rather than the formation of two-phase samples. Our XRD and EDS data obtained for samples with higher Ag-content, Ag-2 up to Ag-3, support this literature hypothesis. However, at low content of silver in HPW as for Ag-0.5–Ag-1 salts, non-homogeneous distribution of Ag was evidenced by the EDS analysis and in the case of Ag-0.5 the crystalline phase of parent HPW was observed by XRD. No reflexes originating from crystalline HPW were observed at higher content of silver, such as in Ag-1 sample. However, the presence of HPW in the form of amorphous and/or small clusters may be postulated in view of EDS data (Table 2). On the other hand, at higher silver content, such as in Ag-2 sample, the residual acidic phase, $H_3PW_{12}O_{40}$, seems to be more homogeneously distributed throughout the bulk of crystalline particles of the salt. This may be considered as the formation of solid solution, what is consistent with the previous literature reports [21,33].

3.2. Methanolysis experiments

It is well known, that each step of transesterification reaction is reversible. However, Diasakou et al. claimed that the reverse reactions in excess methanol were not important and could be ignored [34]. Therefore, in the present work, all the methanolysis reactions were carried out at the excess of methanol, using initial molar ratio of methanol to triglyceride equal to 29:1.

3.2.1. Transesterification of triacetin with methanol

In this part of our study, silver salts of HPW are examined as the catalysts for transesterification reaction. Therefore, catalytic efficiency of pure $AgNO_3$ was tested as well. Although $AgNO_3$ is soluble in methanol no reaction was observed for both triglycerides: triacetin and castor oil. In order to check the contribution from non-catalytic reaction, blank experiments of triacetin methanolysis were carried out in the absence of catalyst. The conversion of triacetin and the yield to methyl ester obtained in blank run are displayed in Fig. 9. The data show that the reaction carried out with-

Table 3
Methanolysis of triacetin and castor oil in the presence of $H_3PW_{12}O_{40}$ and Ag-salts. The yield to methyl-ester after 30 min of reaction (*Y* [%]) and the ratio of specific activities (SPC) defined as the yield related to 1 g of Ag-salt or $H_3PW_{12}O_{40}$.

Catalyst	Surface area [m^2/g]	Castor oil *Y* [%] 30 min	Triacetin *Y* [%] 30 min	SPC-tact/SPC-cas
HPW	5	23.9	25.7	4.3
Ag-0.5	3.56	21.2	22.7	4.3
Ag-0.75		15.5	20.8	5.3
Ag-1	3.23	10.1	17	6.6
Ag-1.5		7.9	14.2	6.9
Ag-2	4.74	5.6	11	7.4
Ag-2.5	4.05	3.5	7.4	7.8
Ag-3	5.54	0.3	3.6	44

out the catalyst proceeded very slowly and only 0.9% conversion of triacetin was attained after 30 min.

In the presence of all Ag-salts as well as parent $H_3PW_{12}O_{40}$ the transesterification of triacetin with methanol proceeded at different rates. In the catalytic experiments, the same number of moles of parent $H_3PW_{12}O_{40}$ acid and Ag-HPW salts was used. As suggested by Morin et al. [7], prior to catalytic experiment the sample of HPW was dried for 18 h at 230 °C. It is well known that parent $H_3PW_{12}O_{40}$ is readily soluble in methanol and when used in methanolysis experiment acts as homogeneous catalyst. The products distribution profile obtained in the presence of soluble $H_3PW_{12}O_{40}$ is displayed in Fig. 9. The change in reagents concentrations is identical to those commonly observed in the transesterification of triglycerides. First, an initial build-up of the diglyceride intermediates (diacetin), achieving a maximum concentration at time of ca. 60 min takes place. Later, the monoglyceride (monoacetin) product is formed. Glycerol and methyl ester are observed from the very beginning of reaction. Almost identical product distribution profile is observed over Ag-0.5 sample (Fig. 9). The only noticeable difference is the slightly higher content of monoacetin observed over Ag-0.5 sample. Similar products distribution profiles were observed in the presence of other silver salts.

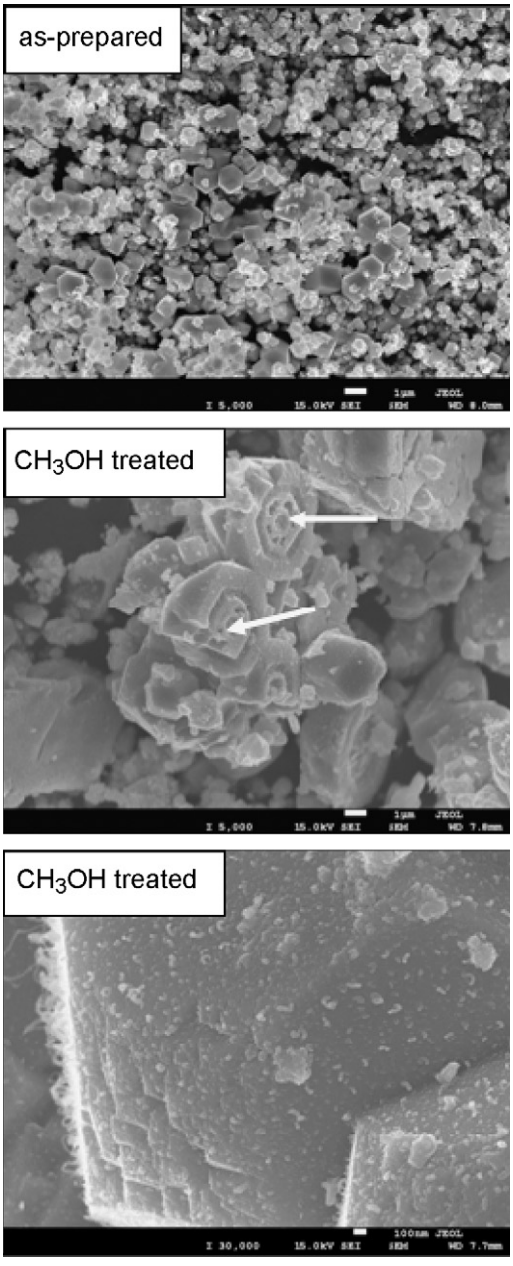

Fig. 8. Scanning electron micrographs of starting Ag-3 salt and the sample treated by methanol.

Catalytic performance of Ag-salts of various Ag-content is compared in Fig. 10 showing the conversion of triacetin against reaction time. It can clearly be seen that the rates of methanolysis differ depending on the content of Ag-cation in HPW. The highest conversion of triacetin is attained in the presence of Ag-0.5 salt and this conversion is only slightly lower than that obtained in the presence of soluble parent HPW. Furthermore, the conversion of triacetin gradually decreases as the protons in HPW are replaced by Ag^+ cations. Methanolysis reaction occurs in the presence of Ag-3 salt as well but at much lower rate (Table 3). It should be noted that catalytic activity of fully substituted Ag-3 salt was also observed by Moffat in dehydration of 1-, 2- and tert-butyl alcohols [20]. The activity of Ag-3 was ascribed by the authors to the residual protons found in the Ag-3 salt even when the Ag-content used for the salt preparation exceeded the stoichiometric value.

However, macroscopic observations showed that catalytic performance of Ag-0.5–Ag-1 salts is different from that of Ag-2, Ag-2.5 ones. When the white powder of Ag-0.5 salt is added to the reaction mixture and then heated up to 50 °C, reaction mixture becomes transparent and practically no presence of solid catalyst is observed. However, after completion the reaction and cooling the mixture to room temperature, the white solid was slowly separated (24 h) from the liquid. Similar behaviour was observed for Ag-1 sample but it did not form completely transparent mixture and the presence of salt powder was always observed. These macroscopic observations also show that Ag-0.5–Ag-1 samples are partially soluble in reaction mixture at 50 °C.

The solids separated after the reactions carried out in the presence of partially soluble Ag-0.5–Ag-1 samples were analyzed by SEM and the obtained images are shown in Figs. 5 and 6, respectively. The results of EDS analysis obtained for these precipitates are given in Table 2. It can be seen that precipitates separated from the reaction mixture are in the form of crystallites. However, their shape and sizes differ remarkably from those of initial Ag-0.5 and Ag-1 samples (Figs. 5 and 6, respectively). Moreover, substantial

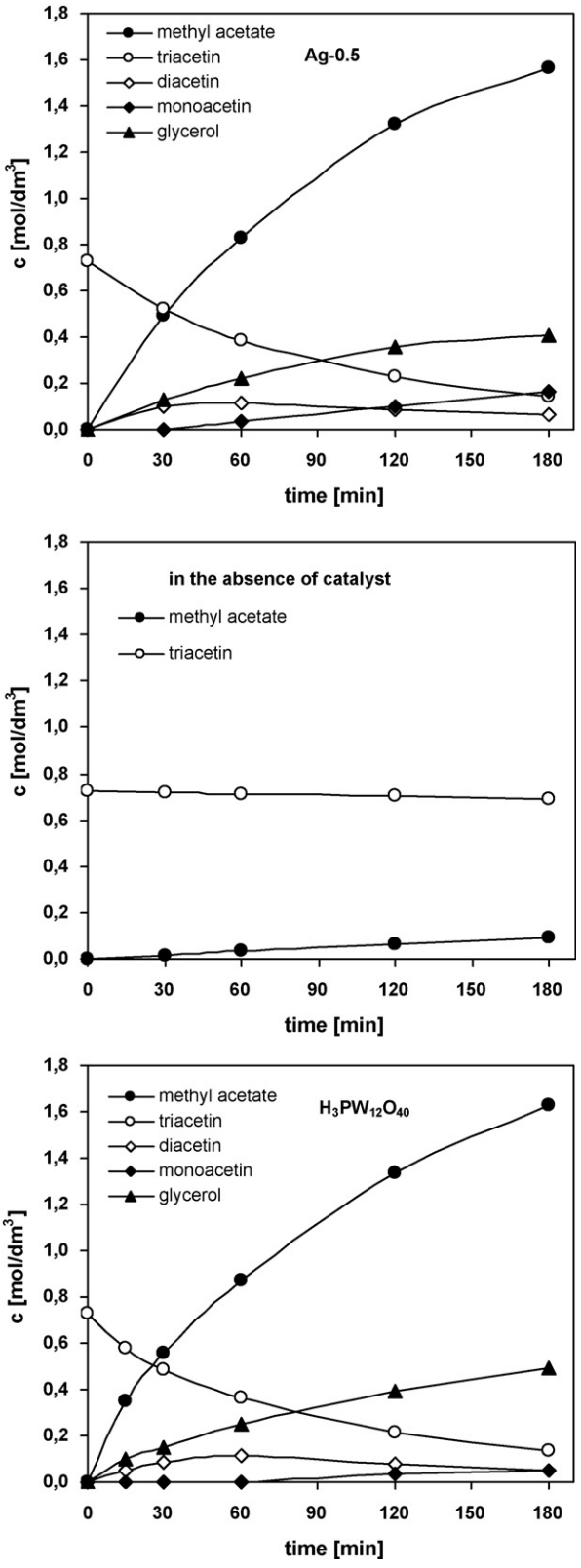

Fig. 9. Reaction profile for methanolysis of triacetin in the presence of Ag-0.5 salt, soluble $H_3PW_{12}O_{40}$ and in the absence of catalyst (reaction conditions: molar ratio, methanol:triacetin = 29:1; catalyst concentration, 0.00225 mol/dm^3; temperature, 50 °C).

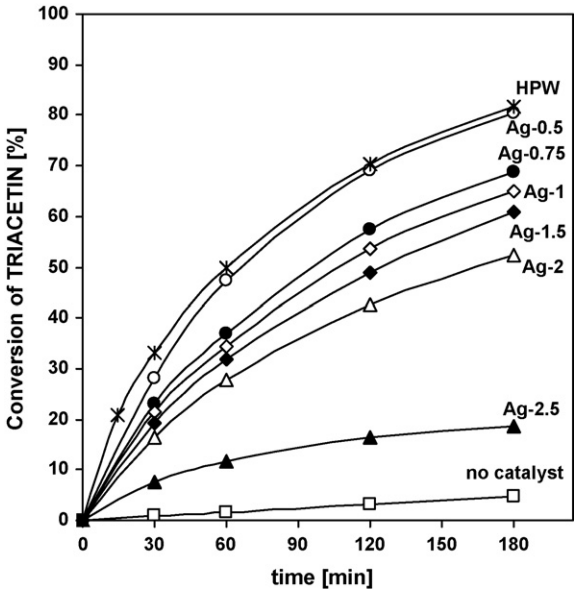

Fig. 10. Conversion of triacetin vs. reaction time in the presence of Ag-salts and soluble $H_3PW_{12}O_{40}$ (reaction conditions: molar ratio, methanol:triacetin = 29:1, catalyst concentration, 0.00225 mol/dm^3, temperature, 50 °C).

differences are also observed in the values of W/Ag ratios. For Ag-1 sample, the initial W/Ag = 6 decreases to ca. 4 after the reaction, i.e. to the value characteristic of fully substituted Ag-3 salt. This may indicate that crystalline HPW present in as-received Ag-1 sample was to some extent dissolved during methanolysis reaction and the white precipitate separated after the reaction was entirely composed of Ag-3 salt. This conclusion is quite well supported by the SEM image (Fig. 6) showing that crystalline particles of precipitate are smaller than those of initial Ag-1 sample and they are of similar sizes/shapes to those of as-prepared Ag-3 salt (Fig. 8).

It is well known that $H_3PW_{12}O_{40}$ is readily soluble in water and methanol. It is very probable that upon contacting of the Ag-0.5 sample with reaction mixture, crystalline heteropolyacid $H_3PW_{12}O_{40}$ (evidenced by its XRD diffraction) leached out by dissolving in methanol. Leaching of HPW seems to be also probable in the case of both Ag-0.75 and Ag-1 samples, because of non-uniform composition of these samples and distinct changes in their morphology (compositions) after the catalytic tests.

It may be supposed that small amounts of "solid" – not dissolved in the reaction mixture – are the insoluble Ag-salts, i.e. the salts with high silver content like Ag-2, Ag-2.5 and most probably Ag-3 one. However, their activity for methanolysis of triacetin is distinctly lower than that of soluble $H_3PW_{12}O_{40}$ (Fig. 10). Therefore, under the reaction conditions, almost all catalytic activity observed in the presence of Ag-0.5–Ag-1 samples may be due to homogeneous rather than heterogeneous catalysts, as a result of HPW leaching.

In contrast to the Ag-0.5–Ag-1 salts, in the course of reactions performed in the presence of Ag-2–Ag-2.5 samples, separate phases of catalysts were observed in the reaction mixtures during the whole catalytic experiments, and the reaction mixture became "milky" at temperature 50 °C. This suggests that these Ag-salts when dispersed in reaction mixture form a colloidal solution. This observation is well supported by the literature reports showing that Cs-salts of HPW readily form colloidal dispersion in polar solvents like water and methanol because they consist of very fine primary crystallites (ca. 10–20 nm in average) [33]. Data reported by Nakato and co-workers [35] as well as our previous results [17] showed that colloidal particles of Cs-salts of HPW of size within the range 50–200 nm were formed in water medium. Here, colloidal

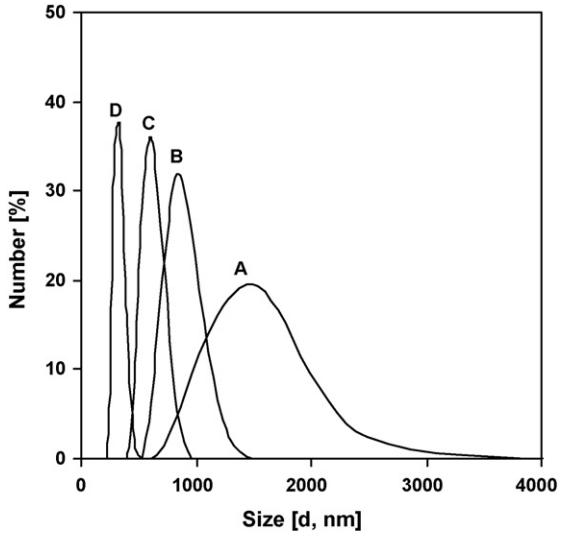

Fig. 11. The size of colloidal particles formed by Ag-2 salts in reaction mixture composed of methanol and triacetin (29:1) determined at different temperatures: A (25 °C, d = 1484 nm), B (35 °C, d = 825 nm), C (45 °C, d = 615 nm) and D (55 °C, d = 342 nm).

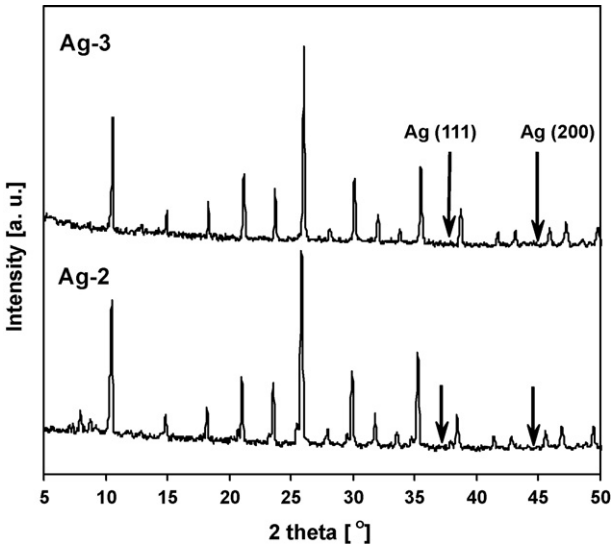

Fig. 12. Powder X-ray diffraction patterns of methanol treated Ag-2 and Ag-3 salts.

dispersion of Ag-2 salt during methanolysis of triacetin is evaluated by the measurements performed by laser diffraction technique (Fig. 11). As described before (Section 2) the measurements were carried for system obtained by introducing Ag-2 salt into the solution composed of methanol and triacetin with a molar ratio of 29:1. They were performed at 25 °C and subsequently after heating the mixture to 35 °C, 45 °C and 55 °C. The size distribution profiles are displayed in Fig. 11. They show the formation of colloidal particles of Ag-2 salt even at room temperature. It can also be seen that the size of colloidal particles remarkably decreases (ca. 5 times) under heating the reaction mixture up to 55 °C (close to the temperature of reaction). The particles of average size of ca. 340 nm are then observed. This indicates that the secondary crystalline particles which are composed of primary particles are to high extent decomposed in polar medium forming colloidal dispersion.

The SEM micrograph of precipitate separated after reaction carried out over Ag-2 salt is reported in Fig. 7. Although the shape and the size of crystallites practically did not change, the formation of small "nanowires" could be observed mostly on the edges of salt crystallites. To identify these changes, the Ag-2 salt was treated by methanol which is known to be a reducing medium towards the silver compounds. Methanol treatment was performed under condition identical to those used in methanolysis of triacetin (3 h at 50 °C). The SEM images registered for the methanol treated sample evidenced changes in the morphology similar to that of Ag-2 salt (Fig. 7). The EDS analysis performed in the areas with "nanowires" shows the W/Ag ratio as high as ca. 2, much lower than the stoichiometric W/Ag = 6. This may indicate that the areas with nanowires are enriched by silver. However, no particles of metallic silver were observed even in the SEM images registered at as high magnification as 200,000 what allows to detect metal nanoparticles of 5–10 nm in size.

Fig. 8 shows micrograph of as-prepared Ag-3 salt (one image) and two representative images of Ag-3 sample treated by methanol. Two images are provided, because of different nature of morphology changes induced by methanol. They are in the form of small new nanowires clearly observable in the first image and micro-regions of "special ordering" like "flowers" reported in the second image.

In the latter regions, similarly as in the areas with nanowires the W/Ag ratio is low, equal to ca. 2 indicating surface enrichment by silver. These changes and particularly the formation of "nanowires" seem to be interesting and studies concerning their characterization are under progress.

Literature data demonstrated that during hydrogen treatment of fully substituted Ag-3 salt at high temperature (215 °C) ionic silver was partially reduced to Ag^0 which formed relatively large crystalline particles observed by the XRD technique [36]. However no microscopic studies were carried out by the authors to evaluate changes in morphology of Ag-3 salt induced by the reduction of ionic Ag^+ by hydrogen.

In Fig. 12 the X-ray diffraction pattern of Ag-salts treated by methanol is displayed. For clarity, the positions of reflexes characteristic of crystalline silver are marked on the diffraction patterns. No XRD peaks originating from crystalline Ag particles are observed. Thus, no crystalline silver was formed after methanol treatment, but the formation of silver nanoclusters cannot be excluded.

From the present microscopic and XRD results it can be concluded that after methanol treatment some changes in morphology of Ag-2 salt are induced and most probably silver ions are partially reduced. To clarify this reduction effect the XPS measurements were carried out. For our studies, the Ag-2 salt has been chosen, because its morphology changed after methanolysis reaction as well as after treatment by methanol (Fig. 7). The XPS spectra of the Ag 3d region in as-received Ag-2 catalyst and the sample after treatment by methanol (for 3 h at 50 °C) are displayed in Fig. 13. The binding energies of the Ag $3d_{5/2}$ states and their contributions to the whole Ag-peak are collected in Table 4.

According to the literature data, the binding energy of the Ag $3d_{5/2}$ signal for silver states Ag^+ (as in Ag_2O) and Ag^{2+} (as in AgO), are 367.8 eV and 367.4 eV, respectively. Higher binding energies of 368.3–368.7 eV are reported for Ag^0 (metallic) state [37]. How-

Table 4
XPS analysis data for Ag-2 salts, as-received sample and the sample treated by methanol. Surface concentrations (in at.%) and binding energies for Ag $3d_{5/2}$ peaks.

Sample	Ag (at.%)	W (at.%)	W/Ag	B.E of Ag $3d_{5/2}$ [eV]
Ag-2 as-received	3.2	17.1	5.3	366.7 (2.2%) 368.3 (90.5%) 369.5 (7.3%)
Ag-2 treated by methanol	2.6	16.3	6.3	366.5 (2.3%) 368.4 (65.0%) 369.5 (26.6%) 371.6 (6.1%)

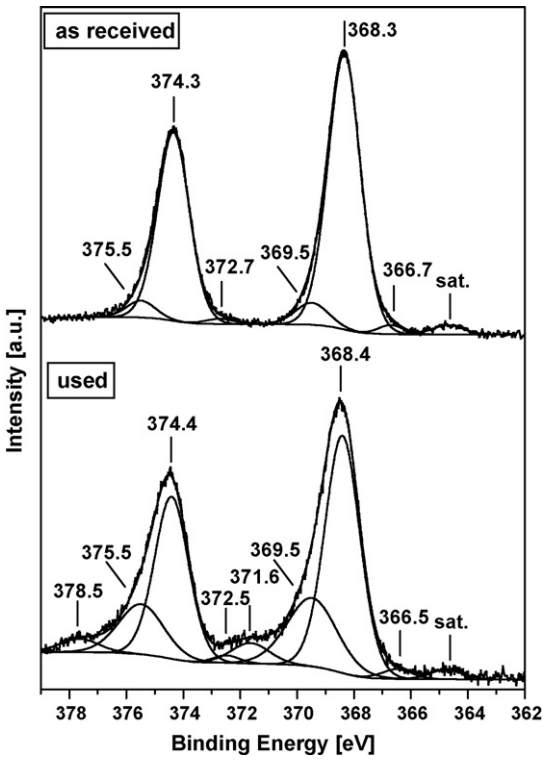

Fig. 13. XPS Ag 3d spectrum of starting and methanol treated Ag-2 catalyst.

ever, literature reports claim that it is difficult to assign the binding energies for Ag $3d_{5/2}$ peaks in the case of the samples consisting of silver dispersed in carrier matrices because their XPS signals could change due to different support interactions.

For instance, in few studies, the binding energies for Ag $3d_{5/2}$ as high as ca. 370 eV, i.e. higher than those reported in the XPS reference data [38] were observed. Such higher energies were determined for Ag/Al_2O_3 catalysts [39,40] as well as Ag/Au core–shell nanoparticles [41]. Although this high binding energy was considered as indicative of the presence of strong electronic interactions between carrier and silver, their nature has not been discussed in more detail. Moreover, the shift of BE of Ag^0 state was also observed for Ag/ZnO particles due to strong silver–support interactions [42].

In the spectrum of as-received Ag-2 salt, the Ag $3d_{5/2}$ region shows two distinct peaks components, a large and dominating centred at 368.3 eV (90.5%) and a smaller one at higher energy of 369.5 eV (7.3%) (Fig. 13). A small peak of energy ca. 366.5 eV (2.2%) shows some traces of unidentified silver species.

In view of literature data, the former XPS signal could be ascribed to Ag^+ ions. The binding energy of 369.5 eV is too high to be assigned simply to the bulk metallic silver. According to the literature reports this energy may indicate the presence of silver nanoclusters interacting with carrier material, the nature of which cannot be speculated at the moment. They may be considered as formed in the initial Ag-2 sample due to photochemical reaction.

Thus, in initial Ag-2 salt silver appears mostly in the form of ionic Ag^+ and a small amount of silver species. The treatment of Ag-2 with methanol resulted in some changes in the Ag $3d_{5/2}$ peak. As shown in Fig. 13 the contribution of peak originating from ionic silver decreases (from 90.5% to 65%) whereas the shares of highly energetic silver peaks at binding energies of 369.5 eV and 371.6 eV grow. This indicates that after methanol treatment the content of ionic Ag^+ silver decreases at the surface of Ag-2 salt at the expense of the Ag^0-species, most probably Ag-nanoclusters interacting with the support. The amount of metallic silver increased ca. 4 times on the surface of Ag-2 salt after methanol treatment (from 7.3% to 26.6%, Table 4). Hence, from XPS, electron microscopic images and EDS data it may be supposed that partial reduction of ionic silver and the presence of "nanowires" are to some extent mutually occurring phenomena.

3.2.2. Transesterification of castor oil

In catalytic experiments, the reactivity of Ag-salts for transesterification of triacetin, a short-chain triglyceride, is compared to that for natural oil, i.e. castor oil. As described before, in both systems composed of methanol – castor oil and methanol – triacetin, the homogeneity of the reaction mixtures was attained and no separate phases of triglycerides and methanol appeared.

In the selected catalytic experiments for castor oil the composition of reaction mixture against reaction time was determined by HPLC techniques. For all of the investigated catalysts the content of triglycerides in the reaction mixture decreased with time, whereas no remarkable peaks originating from di- and mono-glycerides were observed. Therefore, in the discussion of catalytic results the yield to methyl-esters formed under methanolysis of castor oil is taken into account, identically to the procedure widely used in the case of natural oils. Moreover, as shown in Figs. 1 and 2, apart

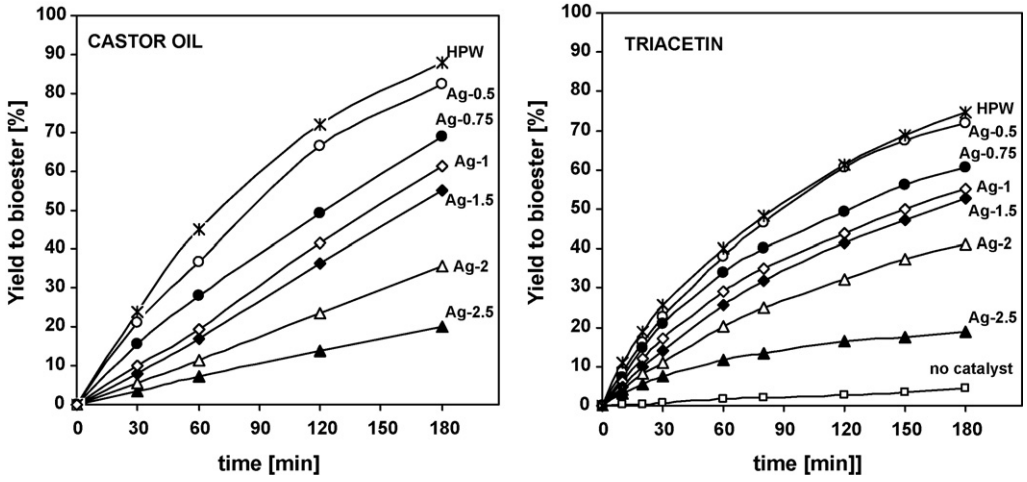

Fig. 14. The formation of methyl-esters (percentage yield *Y*) in the methanolysis of castor oil and triacetin in the presence of Ag-salts. The reaction conditions: initial molar ratio of MeOH/oil = 29:1, the concentration of Ag-salts in reaction of triacetin 0.00225 mol/dm^3, in reaction of castor oil 0.012 mol/dm^3.

from the dominating triglycerides of ricinoleic acid, low amount of triglycerides of other fatty acids is also present in castor oil, making determination of conversion data more complex.

In Fig. 14 the yield to methyl-esters against reaction time is reported. The data obtained in the presence of Ag-salts are compared to that obtained in the presence of soluble, parent $H_3PW_{12}O_{40}$ acid. For the comparison, the yields to methyl-ester obtained in reaction for triacetin are also displayed in Fig. 14. It should be mentioned that the concentration of Ag-salts (and HPW) used in experiments for castor oil (0.012 mol/dm^3) was ca. 5 times higher than that of the reaction for triacetin (0.00225 mol/dm^3).

The effects observed for transesterification of castor oil are similar to those for triacetin. The Ag-0.5–Ag-1 samples were partially soluble in the reaction mixture whereas the Ag-2, Ag-2.5 salts formed separate phases, colloidal dispersions. Similarly to the transesterification of triacetin, that is at the same number of moles of HPW and Ag-0.5 salt in the reactor, the yield to methyl-esters in the presence of Ag-0.5 salt is only slightly lower than that obtained in the presence of homogeneously acting $H_3PW_{12}O_{40}$ acid. Among the Ag-salts, the yield to methyl-esters gradually decreases as protons in HPW are replaced by Ag^+ cation.

The micrographs of precipitates separated after the reaction of castor oil are displayed in Figs. 5–7 and the data of EDS analysis are collected in Table 2.

It is observed that the morphology of precipitates separated after the reaction remarkably differs from that of as-received samples. The well-shaped crystalline particles of initial salts become like "gel-type" material (Figs. 5–7) particularly in the case of spent salts with high content of silver. For Ag-0.5 sample, only small part of crystalline particles is in the "gel" form (Fig. 5). The relative content of "gel-type" material increases as the content of Ag grows and spent Ag-2 salt appears like a "piece of gel" (Fig. 7).

Thus, it can clearly be seen that when colloidal dispersion of Ag-salts was cooled in contact with reaction mixture composed of tri-, di- and mono-glycerides, glycerol, methyl-esters and methanol the effect of particles aggregation to form "gel-type" structures was noticed. It should be stressed that this effect was not observed when a short-chain triglyceride, triacetin, was used.

In order to examine the reason of "gel-type" material formation by spent Ag-samples and taking into account that methanol is one of the reactant, the Ag-2 salt was prepared using methanol solutions of reagents (HPW and $AgNO_3$) instead of commonly used aqueous solutions. However, in methanol medium Ag-2 salt was obtained in the form of well-shaped crystalline particles and no "gel-type" aggregates were formed. Moreover, no "gel-type" structures were observed for spent Ag-salts after their use for methanolysis of triacetin. Therefore, it can be concluded that the aggregation of colloidal particles of Ag-salts to form "gel-type" materials is facilitated by the presence of castor oil, i.e. long-chain glycerides.

In Table 2 the results of EDS analysis for Ag-salts after the reaction of castor oil are summarized. For initial Ag-0.5 salt and the precipitate obtained after the reaction the values of W/Ag ratio are observed within a wide range showing high non-homogeneity of the samples.

However, for Ag-1 sample, the initial W/Ag = 6.1 decreased after the reaction to W/Ag = 4.2 characteristic of Ag-3 salt. This effect is similar to the one observed in methanolysis of triacetin (Table 2). On the other hand, samples with higher content of silver in HPW, i.e. Ag-2 salt, retained the average W/Ag ratios equal to 6 after methanolysis of both triglycerides, castor oil and triacetin. Moreover, no "nanowires" or metallic silver particles were observed in precipitates separated after the reaction of castor oil performed in the presence of Ag-2, Ag-2.5 and Ag-3 salts even on the SEM images registered at very high magnification (200,000×). This indicates that long-chain triglycerides can block the formation of "nanowires".

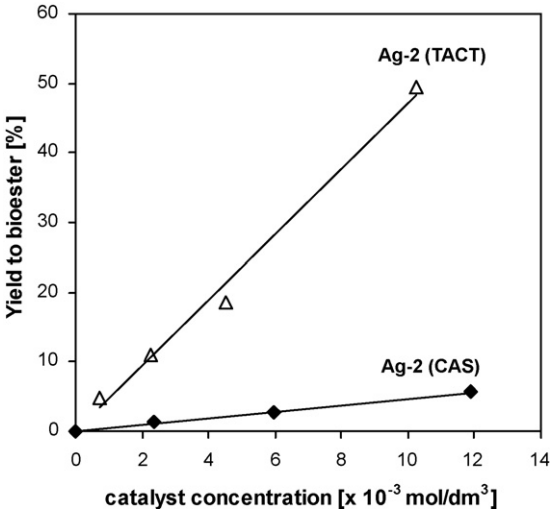

Fig. 15. The yield to methyl-esters (*Y*, %) after 30 min of reaction vs. the concentration of Ag-2 salt, methanolysis of triacetin (TACT) and castor oil (CAS).

In Table 3 the yields to methyl-esters obtained in transesterification of triacetin, a short-chain triglyceride and in reaction of castor oil comprising long-chain triglycerides are compared. It should be stressed that the concentration of Ag-salts (and HPW) in experiments of castor oil was ca. 5 times higher than that in the reaction for triacetin.

For the Ag-2 salt the influence of its concentration in reaction mixture on the yield to bio-ester was examined and the obtained results are plotted in Fig. 15. It is observed that in methanolysis of both triglycerides, the yield to bio-ester [*Y*, %] increases when the concentration of Ag-2 salt in solution grows. The observed linear increase of *Y* against the amount of Ag-2 salt indicates that external mass-transport effect does not affect activity.

Fig. 16 displays the relationships between the contents of Ag per Keggin unit and the yields to methyl-esters (obtained after 30 min of reaction related to 1 g of salt). Curve TACT corresponds

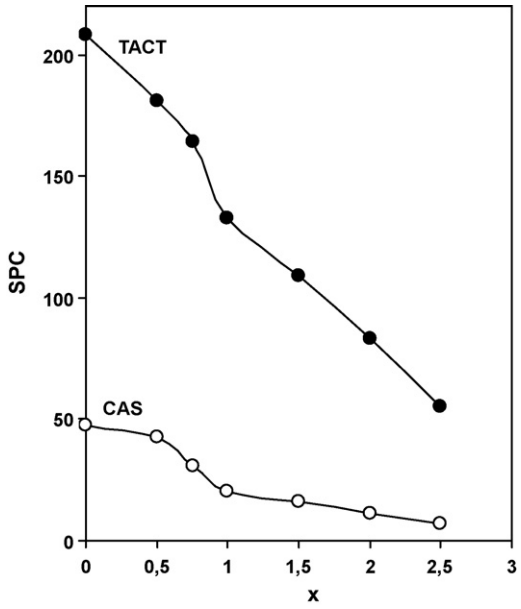

Fig. 16. Specific activity of HPW and Ag-salts (defined as the yield to methyl-esters after 30 min of reaction related to 1 g of salt or HPW) as a function of number of Ag^+ cation (*x*) in the salt. Methanolysis of castor oil (CAS-curve) and triacetin (TACT-curve).

to methanolysis of triacetin, and curve CAS shows the results for methanolysis of castor oil. Similarly to what was reported by other authors methanolysis of triacetin, short-chain triglyceride, is faster than that of castor oil comprising long-chain triglycerides. This is observed in the presence of soluble $H_3PW_{12}O_{40}$ as well as all Ag-salts.

However, under conditions of homogeneous catalysis as in the case of soluble $H_3PW_{12}O_{40}$ and highly soluble Ag-0.5 sample, transesterification of triacetin is ca. 4.3 times faster than that of castor oil (Table 3). The difference between the rates for short and long-chain triglycerides successively increases when the content of Ag in silver salts grows. Finally, in the presence of Ag-2 and Ag-2.5 catalysts transesterification of triacetin is ca. 7.4–7.8 times faster than that of castor oil.

To explain this effect some differences between homogeneously and heterogeneously catalysed transesterification are taking into consideration. It may be thought that in the case of heterogeneously acting catalyst, the accessibility of larger, long-chain triglyceride molecules to the active sites of solid catalyst is more difficult than in the case of soluble catalysts. This may result in less effective utilization of active centres in solid catalyst during reaction of castor oil than in the case of triacetin, a short-chain triglyceride. Moreover, it is generally accepted that in transesterification reaction catalysed by acid catalysts, the triglyceride molecules are adsorbed by H^+ centres of catalyst to form protonated carboxylic groups and they react with methanol coming from the bulk of liquid [1]. Triglycerides of castor oil are larger molecules and it may be thought that it is more difficult for methanol molecules to reach the protonated carboxylic group when there is a large alkyl chain from castor oil blocking the access. In the case of solid catalyst, this may also lead to lowering the rate for larger triglycerides relative to that for short molecules. Hence, the larger difference between the rates for short and long-chain triglycerides observed in the presence of Ag-2–Ag-2.5 salts compared to homogeneously catalysed reactions suggests higher contribution of heterogeneous catalysis for the salts with high Ag-loading, such as Ag-2 and Ag-2.5.

It cannot be excluded that more restricted access of methanol to the surface of Ag-salts in the case of castor oil may also explain the lack of Ag^+ reduction leading to the formation of "nanowires", the effect observed in methanolysis of triacetin (Figs. 7 and 8).

Reusability of catalyst is one of the most important features of a heterogeneous catalyst for its commercialization. Here, distinct changes in morphologies of Ag-3 and Ag-2 samples after the catalytic tests are observed. The samples were in the form of gel, what makes almost impossible their quantitative separation from the reaction mixture to perform the reusability catalytic test. It cannot be excluded that although "gel-type" morphology is formed, it does not exert their acidic properties responsible for the catalytic activity. However, it must influence their specific surface area, the next parameter determining catalytic activity. Another possibility is that some of reaction products, like glycerol and partial glycerides are accumulated by "gel-type" material and it may cause some changes in the catalytic activity for recovered samples. All of these phenomena indicate reuse of Ag-2, Ag-3 salts do not provide informative results.

As described before, Cs-, K- and Ag-salts of HPW form colloidal suspension in polar medium such as water or alcohol because they consist of ultrafine crystallites (ca. 10–20 nm in average) and recovering of the catalysts is not easy by means of simple filtration and/or centrifugation. This problem has already been encountered in number of previous papers reporting preparation and characterization of K- and Cs-salts of HPW [32,35,43] as well as in quite recently published paper devoted to catalytic activity of Cs-salts in transesterification of vegetable oil [15]. The authors [15] demonstrated that in transesterification of rapeseed oil with ethanol over $Cs_2HPW_{12}O_{40}$ (under mild conditions) it was impossible to make re-using catalytic tests because it was impossible to get a perfect translucent phase using successive centrifugation/filtration of Cs-catalyst (although the conversion of oil in such experiment attained ca. 5% only). Finer particles of the acidic cesium salt remained in the suspension due to their size as small as 10–30 nm [15]. However, from TGA-DTA and XRD measurements performed for as-received and used $Cs_2HPW_{12}O_{40}$ catalysts the authors supposed about a relative good resistance of $Cs_2HPW_{12}O_{40}$ to the leaching in reaction medium – ethanol.

On the other hand, the reuse of cesium salts $Cs_xH_{4-x}SiW_{12}O_{40}$ ($x = 2.5$–4) was examined by Pesaresi et al. [16] in transesterification of tributyrin (C_4), a model short triglyceride molecule. The authors reported that after hot filtration, the catalysts could be recycled three times without loss of activity (the activity decreased by 10–20%). A short information about a reuse of $Cs_xH_{3-x}PW_{12}O_{40}$ catalysts ($x = 2$–2.3) with no leaching of soluble HPW in transesterification of tributyrin was mentioned by Narashimharao et al. [13]. However, no data from reuse of the catalysts were reported. The authors claimed also that Cs-salts with higher Cs content were stable under methanol reflux, but no experimental evidence proving this stability was reported [13].

Moreover, numerous papers published by Okuhara, Misono and co-workers [9,12,44,45] demonstrated that $Cs_{2.5}H_{0.5}PW_{12}O_{40}$ efficiently catalysed reactions performed in the presence of excess of water, like hydrolysis of esters (ethyl acetate, cyclohexyl acetate, 2-methylphenyl acetate, 2-nitrophenyl acetate) and hydration of olefins. Although the $Cs_{2.5}H_{0.5}PW_{12}O_{40}$ is termed as "water tolerant catalyst" its activity in the hydrolysis of ethyl acetate (performed at 60 °C) slowly but continuously dropped during the successive use [12,35]. After five consecutive runs the activity retained ca. 90% of initial value. Moreover, the catalytic activity of Cs-2.5 was reduced by ca. 50% due to pre-treatment with hot water (70–120 °C) before the catalytic experiment. Detailed studies reported by Okuhara and co-workers [12] showed that a small amount of heteropoly species was released into water during the water treatment of Cs-2.5 salt. The liberated species were present as small clusters, retaining essentially the secondary structure of the Cs-2.5 salt, and they were enriched by H^+ ions. Similarly, slow leaching of $Cs_{2.5}H_{0.5}PW_{12}O_{40}$ catalyst during methanolysis of vegetable oil was observed by Chai et al. [14]. After six runs of the catalytic experiment ca. 5.6% of the starting amount of the catalyst was dissolved.

Relative to the present Ag-salts, a "catalyst solubility effect" giving rise to homogeneous catalysis is observed for silver salts of Ag-content $x < 2$. The salts of higher Ag-loading, $x > 2$, exist mostly in the solid state during the methanolysis reaction because the white colloidal dispersion is observed throughout the whole catalytic experiment. However, in their presence some contribution of homogeneous catalysis cannot be excluded. A various procedures such as filtration, and/or successive centrifugation of hot and/or cooled (up to ca. 0 °C) reaction mixture were used to separate these catalysts after the reaction. Although completely transparent solution was obtained after the separation of white precipitate of Ag-2 salt, the presence of Ag^+ ions was detected upon addition of Cl^- ions. Moreover, dropwise addition of ascorbic acid, i.e. the analytical reagent commonly used to test the presence of $PW_{12}O_{40}^{3-}$ ions [46], caused the formation of metallic silver instead of expected blue coloured complex. Thus, it seems very probable that catalytic behaviour of Ag-samples with higher Ag-content (Ag-2–Ag-3) is similar to that observed by Okuhara et al. [44,45] for $Cs_{2.5}H_{0.5}PW_{12}O_{40}$ during hydrolysis of esters. Therefore the "catalyst solubility effect" giving rise to homogeneous catalysis cannot be excluded in the case of Ag-2–Ag-3 samples.

Literature data show that silver salts of $H_3PW_{12}O_{40}$ ($x = 0.5$–3) are efficient catalysts in number of gas-phase reactions such as dehydration of ethanol or butyl alcohols, and hydration of ethylene. The only catalytic reaction performed in liquid phase (in

dichloromethane as the solvent) was the synthesis of β-ketoesters via C–H insertion catalysed by fully substituted Ag-3 salt [23]. Our results indicate that catalytic behaviour of Ag-salts of $H_3PW_{12}O_{40}$ ($x = 0.5–3$) for transesterification of triglycerides, reaction accomplished in polar solvent–methanol, is of higher complexity than gas-phase reactions. The samples with low silver content such as Ag-0.5–Ag-1 are unstable during the transesterification reaction. They partially dissolve in methanol giving a contribution to homogeneous catalysis. On the other hand, the salts with high Ag-content such as Ag-2–Ag-3 are difficult for processing in transesterification of natural triglycerides with methanol.

Due to very fine particles size (primary particles 10–20 nm) they form colloidal dispersion in reaction medium and are hardly separable by filtration/centrifugation after the reaction. Moreover, when used in transesterification of natural oil, they precipitated in the form of "gel-type" material after completion of reaction. As described before, "gel-type" structures were not observed in the case of triacetin, a short-chain triglyceride. Literature data show that Cs-salts of HPW are promising catalysts for the transesterification of natural oils. These conclusions were formulated taking into account their transesterification reactivity for short-chain triglycerides like tributyrin (C_4) while it seems to be not true in the case of vegetable oils.

We decided to report the data showing "strong" changes in the morphology of Ag-salts and particularly the effect of their colloidal state under the conditions of transeterification reaction, due to the presence of methanol. We observed the same colloidal state – and similar problems with other salts, namely Cs, K-salts of HPW. On the other hand, a few published papers reported "highly promising" catalytic performance of Cs-salts in transesterification of triglycerides. There is no information about colloidal state and the problems with filtration or "gel-type" material formation after the reaction. Moreover, no enough data related to their reuse are available. Therefore it seems to be necessary to present a real state of Ag-salts when used in polar (methanol) medium. Although they are known to be in fact very active as solid acid catalysts when used in gas-phase reactions, their "promising" catalytic performance in transesterification seems to be questionable. Accordingly, much better solution of this "morphological-reusability" problem is the immobilization of Ag-salts (and Cs-, K-salts) in oxide matrix like silica, similarly to what was successfully done by Izumi et al. [11] for Cs-salts of $H_3PW_{12}O_{40}$. Immobilization of Cs-salts into silica matrix by means of a sol–gel technique produced catalysts of high and stable activity in the hydrolysis of ethyl acetate performed in water medium and similar studies for Ag-salts are under progress. For the immobilized-Ag-salts, the problem of "gel" formation would be omitted and this would provide possibility for recycling and reuse of the Ag-salts.

4. Conclusions

Methanolysis of natural oil, i.e. castor oil and triacetin, a model compound was studied in the presence of $H_3PW_{12}O_{40}$ and its silver salts $Ag_xH_{3-x}PW_{12}O_{40}$ of various Ag-contents ($x = 0.5$ up to 3). All the Ag-salts formed quite well-shaped crystalline particles. The XRD studies showed the presence of parent crystalline HPW in the Ag-0.5 sample. This was not observed at higher Ag-contents, i.e. for Ag-2, Ag-2.5 samples. Their XRD diffraction patterns showed crystalline phase of the salts only. All the Ag-salts proved to be active catalysts in the transesterification of triglycerides with methanol. Their activity gradually decreased as the content of Ag^+ cation in HPW grew. During methanolysis reaction, the Ag-0.5 and Ag-1 samples were partially soluble in reaction mixture resulting in homogeneous rather than heterogeneous mode of reaction due to $H_3PW_{12}O_{40}$ leaching by dissolving in methanol. In the presence of Ag-samples with silver content higher than 1 such as Ag-2 and Ag-2.5 salts, the contribution of homogeneous catalysis to the overall activity cannot be excluded but seems to be definitively lower. During methanolysis of both triglycerides, the salts were in colloidal dispersion making practically impossible their separation after catalytic test. Catalytic performance of Ag-salts for triacetin, a short-chain triglyceride differed remarkably from that of castor oil comprising natural, long-chain triglycerides. After transesterification of natural oil, castor oil, initially crystalline particles of Ag-salts partially rearranged to "gel-type" material which makes very difficult their further processing. The problem can be solved by immobilization the Ag-2, Ag-2.5 salts on supports matrix and the studies are under progress. Although no "gel-type" particles were formed after reaction of triacetin, some of Ag^+ ions were reduced by methanol to form silver nanoclusters accompanied by the formation of "nanowires".

Acknowledgement

A. Zięba acknowledges a Ph.D. grant of the Polish Academy of Sciences.

References

[1] M. Di Serio, R. Tesser, Lu Pengmei, E. Santacesaria, Energy Fuels 22 (2008) 207.
[2] I.K. Mbaraka, B.H. Shanks, JAOCS 83 (2006) 79.
[3] E. Lotero, Y. Liu, D.E. Lopez, K. Suwannakarn, D.A. Bruce, J.G. Goodwin Jr., Ind. Eng. Chem. Res. 44 (2005) 5353.
[4] S.M. Plentz Meneghetti, M.R. Menghetti, C.R. Wolf, E.C. Silva, G.E.S. Lima, M.A. De Coimbra, J.I. Soletti, S.H.V. Carvalho, JAOCS 83 (2006) 819.
[5] S.M. Plentz Meneghetti, M.R. Menghetti, C.R. Wolf, E.C. Silva, G.E.S. Lima, L. Delira Silva, T.M. Serra, F. Cauduro, L.G. De Olivira, Energy Fuels 20 (2006) 2262.
[6] R. Pena, R. Romero, S. Luz Martinez, M.J. Ramos, A. Martinez, R. Natividad, Ind. Eng. Chem. Res. (2009) (accessible on line).
[7] P. Morin, B. Hamad, G. Sapaly, M.G. Carneiro Rocha, P.G. Pries de Oliveira, W.A. Gonzalez, E. Andrade Sales, N. Essayem, Appl. Catal. A: Gen. 330 (2007) 69.
[8] Y.V. Bokade, G.D. Yadav, Ind. Eng. Chem. Res. (2009) (accessible on line).
[9] T. Okuhara, Appl. Catal. A: Gen. 256 (2003) 213.
[10] A. Corma, A. Martinez, C. Martinez, J. Catal. 164 (1996) 422.
[11] Y. Izumi, M. Ono, M. Kitagawa, M. Yoshida, K. Urabe, Micropor. Mater. 5 (1995) 255.
[12] T. Nakato, M. Kimura, S. Nakata, T. Okuhara, Langmuir 14 (1998) 319.
[13] K. Narashimharao, D.R. Brown, A.F. Lee, A.D. Newman, P.F. Siril, S.J. Tavener, K. Wilson, J. Catal. 248 (2007) 226.
[14] F. Chai, F. Cao, F. Zhai, Y. Chen, X. Wang, Z. Su, Adv. Synth. Catal. 349 (2007) 1057.
[15] B. Hamad, R.O. Lopes de Souza, G. Sapaly, M.G. Carneiro Rocha, P.G. Pries de Oliviera, W.A. Gonzalez, E. Andrade Sales, N. Essayem, Catal. Commun. 10 (2008) 92.
[16] L. Pesaresi, D.R. Brown, A.F. Lee, J.M. Montero, H. Williams, K. Wilson, Appl. Catal. A: Gen. 360 (2009) 50.
[17] A. Zięba, L. Matachowski, E. Lalik, A. Drelinkiewicz, Catal. Lett. 127 (2009) 183.
[18] B.Y. Giri, K. Narasiha Rao, B.L.A. Prabhavathi Devi, N. Lingaiah, I. Suryanarayana, R.B.N. Prasad, P.S. Sai Prasad, Catal. Commun. 6 (2005) 788.
[19] L.R. Pizzio, M.N. Blanco, Appl. Catal A: Gen. 255 (2003) 265.
[20] S. Gao, C. Rhodes, J.B. Moffat, Catal. Lett. 55 (1998) 183.
[21] J. Haber, K. Pamin, L. Matachowski, B. Napruszewska, J. Połtowicz, J. Catal. 207 (2002) 296.
[22] M.A. Parent, J.B. Moffat, Catal. Lett. 48 (1997) 135.
[23] J.S. Yadav, B.V. Subba Reddy, K.V. Purnima, S. Jhansi, K. Nagaiah, N. Lingaiah, Catal. Commun. 9 (2008) 2361.
[24] D.E. Lopez, J.G. Goodwin Jr., D.A. Bruce, E. Lotero, Appl. Catal. A: Gen. 295 (2005) 97.
[25] Y. Liu, E. Lotero, J.G. Goodwin Jr., C. Lu, J. Catal. 246 (2007) 428.
[26] D.E. Lopez, J.G. Goodwin Jr., D.A. Bruce, J. Catal. 245 (2007) 381.
[27] Y. Du, S. Liu, Y. Ji, Y. Zhang, S. Wei, F. Liu, F.-S. Xiao, Catal. Lett. 124 (2008) 133.
[28] G.S. Macala, A.W. Robertson, Ch.L. Johnson, Z.B. Day, R.S. Lewis, M.G. White, A.V. Iretskii, P.C. Ford, Catal. Lett. 122 (2008) 205.
[29] L. Zhang, W. Guo, D. Liu, J. Yao, L. Ji, N. Xu, E. Min, Energy Fuels 22 (2008) 1353.
[30] D. Naviglio, R. Romano, F. Pizzolongo, A. Santini, A. De Vito, L. Schiavo, G. Nota, S.S. Musso, Food Chem. 102 (2007) 399.
[31] D.C. Drown, K. Harper, E. Frame, JAOCS 78 (2001) 579.
[32] T. Okuhara, N. Mizuno, M. Misono, Adv. Catal. 41 (1996) 113.
[33] M.A. Parent, J.B. Moffat, Langmuir 12 (3733) (1996) 19.
[34] M. Diasakou, A. Louloudi, N. Papayannakos, Fuel 77 (1998) 1297.
[35] T. Okuhara, M. Kimura, T. Kawai, Z. Xu, T. Nakato, Catal. Today 45 (1998) 73.
[36] T. Baba, M. Nomura, Y. Ono, Y. Kansaki, J. Chem. Soc. Farady Trans. 88 (1992) 71.

[37] S.M. Magana, P. Quintana, D.H. Aguilar, J.A. Toledo, C. Angeles-Chavez, M.A. Cortes, L. Leon, Y. Freile-Pelegrin, T. Lpez, R.M. Torres Sanchez, J. Mol. Catal. A: Chem. 281 (2008) 192.
[38] NIST Standard Reference Database 20, Version 3.2 (Web Version) National Institute of Standards and Technology, Gaithersburg, 2001.
[39] N. Aoyama, K. Yoshida, A. Abe, T. Miyadera, Catal. Lett. 43 (1997) 249.
[40] E. Seker, J. Cavataio, E. Gulari, P. Lorpongpaboon, S. Osuwan, Appl. Catal. A: Gen. 183 (1999) 121.
[41] S.P. Chandran, J. Ghatak, P.V. Satyam, M. Sastry, J. Colloid Interf. Sci. 312 (2007) 498.
[42] Y. Zheng, Ch. Chen, Y. Zhan, X. Lin, Q. Zheng, K. Wie, J. Zhu, J. Phys. Chem. C 112 (2008) 10773.
[43] J.V. Kozhevnikov, Chem. Rev. 98 (1998) 171.
[44] T. Okuhara, H. Watanabe, T. Nishimura, K. Inumaru, M. Misono, Chem. Mater. 12 (2000) 2230.
[45] T. Okuhara, M. Kimura, T. Nakato, Appl. Catal. 155 (1997) L9–L13.
[46] G.D. Yadav, V.V. Bokade, Appl. Catal. 147 (1996) 299.